Preparation, Crystal Structure at 298 and 90 K and Phase Transition in $(C_2H_5NH_3)_2[SbBr_5]$ Studied by the Single Crystal X-Ray Diffraction Method

Maciej Bujak, Bartosz Zarychta, Aleksandra Kobel, and Jacek Zaleski

Institute of Chemistry, University of Opole, Oleska 48, 45-052 Opole, Poland

Reprint requests to Prof. J. Zaleski. Fax: (0048)-77-4410741. E-mail: zaleski@uni.opole.pl

Z. Naturforsch. **59b,** 298 – 304 (2004); received October 24, 2003

The reaction of antimony(III) oxide with ethylamine, in molar ratios from 1:1 to 1:10, in concentrated hydrobromic acid leads to the formation of one product – bis(ethylammonium) pentabromoantimonate(III). The structure of $(C_2H_5NH_3)_2[SbBr_5]$ was determined at 298 and 90 K, below and above the phase transition that occurs at about 158.5 K. The orthorhombic system was found in both phases, space groups *Cmca* and *Pbca* at 298 and 90 K, respectively. At both temperatures the structure consists of $[SbBr_6]^{3-}$ octahedra connected *via cis* bromine atoms forming one-dimensional zig-zag $[\{SbBr_5\}^{2-}]_n$ chains. The ethylammonium cations fill the space between polyanionic chains. The organic and inorganic substructures are held together by a system of N(–H)$\cdots$Br interactions. Their influence on the deformation of $[SbBr_6]^{3-}$ octahedra is well reflected in differences in the corresponding Sb–Br bond lengths and Br–Sb–Br angles in both phases. The phase transition is of the first order and the order-disorder type. It is related to changes in the molecular dynamics of the ethylammonium cations. In the low-temperature phase the organic cations are ordered, while at 298 K both crystallographically independent cations are disordered. The type of disorder is realized by the presence of two positions of the methyl carbon atoms.

Key words: Bromoantimonates(III), Ethylammonium Cation, Phase Transition, Octahedral Distortion

Introduction

This paper forms a part of our larger project relating to the synthesis, structure, phase transitions and molecular motions in the group of new ferroic crystals – halogenoantimonates(III) and halogenobismuthates(III) with organic cations of various sizes and symmetries. Our interest is directed towards the presence of phase transitions, and their mechanisms, and the deformation of the polyhedral coordination sphere about the antimony(III)/bismuth(III) atoms [1 – 5].

We have recently reported the structures and properties of two different chloroantimonates(III) with ethylammonium cations: $(C_2H_5NH_3)_2[SbCl_5] \cdot (C_2H_5NH_3)Cl$ [6] and $(C_2H_5NH_3)_3[Sb_2Cl_9] \cdot (C_2H_5NH_3)[SbCl_4]$ [7]. These compounds were obtained by changing the ratio of antimony(III) chloride to ethylamine between 1 : 0.4 and 1 : 9.5 in aqueous hydrochloric acid solution. In the structure of $(C_2H_5NH_3)_2[SbCl_5] \cdot (C_2H_5NH_3)Cl$ the $[SbCl_6]^{3-}$ octahedra share *cis* edges forming isolated $[Sb_2Cl_{10}]^{4-}$ anions, whereas the structure of $(C_2H_5NH_3)_3[Sb_2Cl_9] \cdot (C_2H_5NH_3)[SbCl_4]$ consists of an anionic substructure composed of two different infinitive zig-zag chains. One is built of $[Sb_2Cl_9]^{3-}$ units, corner sharing octahedra, and the other one is made of the $[SbCl_5]^{2-}$ square pyramids also connected *via* corners. In both structures the ethylammonium cations located between the inorganic moieties are bound to the polyanions by a system of N–H$\cdots$Cl hydrogen bonds.

In the salt $(C_2H_5NH_3)_3[Sb_2Cl_9] \cdot (C_2H_5NH_3)[SbCl_4]$ one phase transition of the first order and the order-disorder type at 274 K has been found. The mechanism of the phase transition is most probably connected with the freezing of the reorientation motions of at least one out of three disordered, crystallographically non-equivalent, ethylammonium cations.

It was also noticed, especially in the case of $(C_2H_5NH_3)_2[SbCl_5] \cdot (C_2H_5NH_3)Cl$, that deformation of the octahedral coordination of the central Sb^{III} atom is among other things related to the presence of the N–H$\cdots$Cl hydrogen bonds between organic and inorganic substructures.

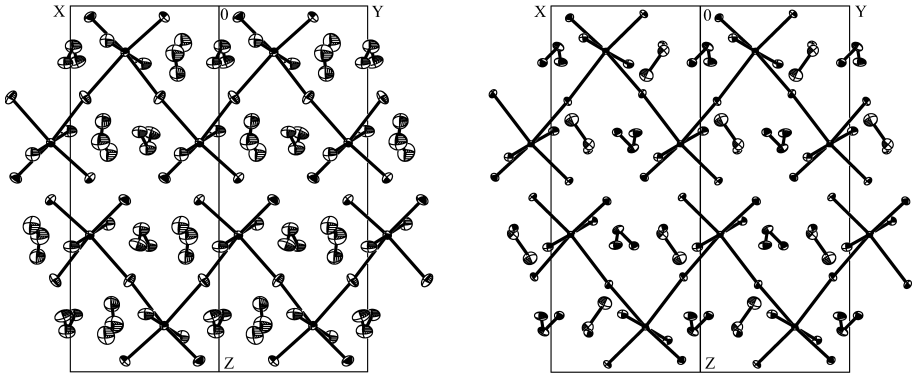

a b

Fig. 1. The packing diagrams of bis(ethylammonium) pentabromoantimonate(III) at 298 K (a) and 90 K (b) projected on the (110) plane (one orientation of the disordered $(C_2H_5NH_3)^+$ cations at 298 K and the hydrogen atoms at 90 K are omitted for clarity). Displacement ellipsoids are plotted at the 25% and 50% probability level at 298 and 90 K, respectively.

In order to obtain further information about the mechanisms of phase transitions as well as the effect of halogen substitution and interactions between organic and inorganic substructures on the type and deformation of anionic halogenoantimonate(III) polyhedra, in this work we have prepared the bromine analogue to study its structure and properties.

Results and Discussion

Preparation and characterization

Bromoantimonates(III) with a wide variety of organic cations defined by the general formula $R_aSb_bBr_c$ (R – organic cation, *a*, *b*, *c* – stoichiometric coefficients) have been synthesized [8–11] and characterized by physicochemical methods including IR, Raman, TGA, DTA, and X-ray techniques [12–15].

The yellow and orange crystals, varying somewhat in shade, may be obtained by mixing solutions of the organic substance and antimony(III) oxide (bromide) in an excess of hot hydrobromic acid. It should be stressed that depending on the type of starting materials, the conditions, and the methods of a synthesis, products of different stoichiometries may crystallize [11].

We tried to obtain all possible products in the reaction of antimony(III) oxide and ethylamine in concentrated hydrobromic acid, changing the molar ratio of reagents between 1:1 and 1:10 (molar ratio of antimony(III) atom to ethylamine). Only one yellow, needle-shaped product – bis(ethylammonium) pentabromoantimonate(III) – was obtained, which crystallizes in the whole studied range of molar ratios.

The same results – formation of only one type of bromoantimonate(III) irrespective of the molar ratio of reactants – were reported by R. D. Whealy and R. L. Yeakley [9]. N. K. Jha and S. S. A. Rizvi reported [11] that the following equilibria exist in aqueous HBr containing amine hydrobromide and antimony(III) bromide:

$$SbBr_3 + Br^- \Leftrightarrow [SbBr_4]^-$$
$$2[SbBr_4]^- + Br^- \Leftrightarrow [Sb_2Br_9]^{3-}$$
$$[SbBr_4]^- + Br^- \Leftrightarrow [SbBr_5]^{2-}$$
$$[SbBr_5]^{2-} + Br^- \Leftrightarrow [SbBr_6]^{3-}$$

Therefore it is difficult to predict which type of bromoantimonate(III) will crystallize. The authors suggested that only the least soluble product is obtained for a given amine hydrobromide.

Our results confirm the formation of one, probably the last soluble, type of salt in the relatively wide range of molar ratio. There are a few examples in the literature where two or three different products were obtained using in the synthesis the same starting materials [*e. g.* 13, 16, 17]. The formation of only one product seems to be mainly related to the specific conditions of the synthesis and type of the organic cation [18].

The bis(ethylammonium) pentabromoantimonate (III) salt has a limited thermal stability. On the basis of TGA studies the powder sample starts to decompose above 450 K.

Crystal structures at 298 and 90 K

The structure of $(C_2H_5NH_3)_2[SbBr_5]$ was determined at 298 and 90 K. At both temperatures crys-

Table 1. The crystal data, X-ray measurements and structure determination summary for $(C_2H_5NH_3)_2[SbBr_5]$ at 298 and 90 K.

	298 K	**90 K**
Empirical formula	— $C_4H_{16}Br_5N_2Sb$ —	
Formula weight	— 613.49 —	
Crystal colour; habit	— yellow; needle —	
Crystal size (mm^3)	$0.22\times0.20\times0.10$	$0.25\times0.18\times0.18$
Crystal system	— orthorhombic —	
Space group	*Cmca*	*Pbca*
Unit cell dimensions (Å)	$a = 7.815(2)$	$a = 7.684(2)$
	$b = 22.301(4)$	$b = 22.413(4)$
	$c = 18.100(4)$	$c = 17.780(4)$
Volume ($Å^3$)	3154.5(12)	3062.1(12)
Z	8	8
Density, calcd. ($g\cdot cm^{-3}$)	2.584	2.661
—, measured ($g\cdot cm^{-3}$)	2.58(1)	–
Wavelength (Å)	— Mo-K_α, $\lambda = 0.71073$ —	
Absorption coeff. (mm^{-1})	14.383	14.817
$F(000)$	2240	2240
θ-Range (°)	3.56 – 29.96	3.41 – 29.71
Index ranges	$-8 \le h \le 10$;	$-24 \le h \le 24$;
	$-29 \le k \le 31$;	$-6 \le k \le 10$;
	$-24 \le l \le 24$	$-31 \le l \le 31$
Reflections	12611/2338	22602/4071
collected/unique	($R_{int} = 0.067$)	($R_{int} = 0.044$)
Observed refls [$I > 2\sigma(I)$]	1331	2896
Data/parameters	2338/75	4071/116
Goodness of fit on F^2	0.869	1.000
Final R indices	$R_1 = 0.036$,	$R_1 = 0.027$,
[$I > 2\sigma(I)$]	$wR_2 = 0.082$	$wR_2 = 0.047$
R Indices (all data)	$R_1 = 0.084$,	$R_1 = 0.048$,
	$wR_2 = 0.094$	$wR_2 = 0.053$
Largest diff. Peak	0.69 and −0.72	1.13 and −1.08
and hole ($e\cdot Å^{-3}$)		

tals are orthorhombic, but at 298 K the space group is *Cmca*, whereas at 90 K it is *Pbca*. In both phases the anionic substructure of $(C_2H_5NH_3)_2[SbBr_5]$ is composed of distorted $[SbBr_6]^{3-}$ octahedra that share two *cis* corners with two other neighbours, forming infinite one-dimensional $[\{SbBr_5\}^{2-}]_n$ chains. The ethylammonium cations are located between the inorganic chains, with their ammonium groups facing the oppositely charged inorganic polyanions. The setting of the cell at 90 K, the asymmetric units of the unit cells, and the labeling of atoms at 298 and 90 K have been chosen to show the structural relationship between positions of corresponding atoms in both phases. It is also obvious from projections of the packing diagrams (Fig. 1).

The crystal data and the structure determination details for $(C_2H_5NH_3)_2[SbBr_5]$ at 298 and 90 K are listed in Table 1. The final atomic coordinates and equivalent isotropic displacement parameters for non-H atoms in both phases are shown in Table 2. The bond lengths, angles, the shortest contacts between organic and inorganic moieties and the hydrogen bond geometries are presented in Tables 3 – 5, respectively.

Table 2. Atomic coordinates ($\cdot10^4$) and equivalent isotropic displacement parameters ($Å^2\cdot10^3$) for non-hydrogen atoms of $(C_2H_5NH_3)_2[SbBr_5]$ at 298 and 90 K.

Atom		x	y	z	U_{eq}[a]
298 K:					
Sb1	8*f*	0	6314(1)	8737(1)	42(1)
Br1	16*g*	2495(1)	6171(1)	9702(1)	71(1)
Br2	8*e*	1/4	6492(1)	3/4	84(1)
Br3	8*f*	0	7528(1)	9054(1)	81(1)
Br4	8*f*	0	5089(1)	8422(1)	84(1)
N1	8*f*	1/2	4672(3)	11555(4)	79(2)
C1	8*f*	1/2	5222(5)	11108(6)	99(4)
C2[b]	16*g*	5320(90)	5761(6)	11530(6)	96(16)
N2	8*f*	1/2	7407(5)	9003(7)	137(4)
C3	8*f*	1/2	7955(9)	8708(10)	157(6)
C4[b]	16*g*	5430(40)	8220(9)	8150(10)	128(11)
90 K:					
Sb1	8*c*	−10(1)	6316(1)	8764(1)	10(1)
Br1	8*c*	2402(1)	6187(1)	9784(1)	16(1)
Br2	8*c*	2682(1)	6559(1)	7603(1)	18(1)
Br3	8*c*	−316(1)	7505(1)	9127(1)	16(1)
Br4	8*c*	281(1)	5086(1)	8416(1)	19(1)
Br11	8*c*	−2654(1)	6097(1)	9678(1)	16(1)
N1	8*c*	5256(5)	4695(2)	11549(2)	20(1)
C1	8*c*	4733(6)	5233(2)	11111(2)	23(1)
C2	8*c*	5129(7)	5791(2)	11531(3)	29(1)
N2	8*c*	5185(5)	7323(2)	8926(2)	20(1)
C3	8*c*	4522(6)	7938(2)	8776(3)	25(1)
C4	8*c*	5403(6)	8205(2)	8111(3)	38(1)

[a] U_{eq} is defined as one third of the trace of the orthogonalized U_{ij} tensor; [b] disordered methyl carbon atoms.

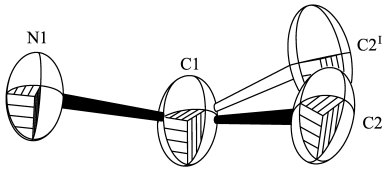

Fig. 2. The disordered ethylammonium cation in the structure of bis(ethylammonium) pentabromoantimonate(III) at 298 K. Displacement ellipsoids are plotted at the 25% probability level. Symmetry code: (I) $-x+1,y,z$.

Structure at 298 K

The central antimony(III) atom located at the special position is surrounded by four crystallographically independent bromine ligands to form a $[SbBr_6]^{3-}$ octahedron. The infinitive $[\{SbBr_5\}^{2-}]_n$ chains are extended along the *a* direction of the unit cell. The longest Sb–Br bonds correspond to bridging bromine atoms and the shortest to terminal, opposite to the bridging ones. The longest Sb–Br distances are

Table 3. Selected bond lengths (Å) and angles (°) for $(C_2H_5NH_3)_2[SbBr_5]$ at 298 K and 90 K.

298 K		90 K	
Sb1–Br1	2.636(1)	Sb1–Br1	2.609(1)
		Sb1–Br11	2.648(1)
Sb1–Br2	2.998(1)	Sb1–Br2	2.972(1)
		Sb1–Br2^{II}	3.057(1)
Sb1–Br3	2.769(1)	Sb1–Br3	2.753(1)
Sb1–Br4	2.790(1)	Sb1–Br4	2.835(1)
N1–C1	1.47(1)	N1–C1	1.490(5)
C1–C2	1.45(2)	C1–C2	1.488(6)
N2–C3	1.33(2)	N2–C3	1.493(6)
C3–C4	1.22(2)	C3–C4	1.488(6)
Br1–Sb1–Br1^{I}	95.38(4)	Br1–Sb1–Br11	95.61(2)
Br1–Sb1–Br2	91.65(2)	Br1–Sb1–Br2	90.49(2)
		Br11–Sb1–Br2^{II}	94.35(2)
Br1–Sb1–Br2^{II}	172.97(2)	Br1–Sb1–Br2^{II}	169.83(2)
		Br11–Sb1–Br2	173.83(2)
Br1–Sb1–Br3	88.94(2)	Br1–Sb1–Br3	90.29(2)
		Br11–Sb1–Br3	88.28(2)
Br1–Sb1–Br4	90.95(2)	Br1–Sb1–Br4	89.31(2)
		Br11–Sb1–Br4	90.80(2)
Br2–Sb1–Br2^{II}	81.33(2)	Br2–Sb1–Br2^{II}	79.58(2)
Br2–Sb1–Br3	91.42(3)	Br2–Sb1–Br3	92.60(2)
		Br2^{II}–Sb1–Br3	87.98(2)
Br2–Sb1–Br4	88.70(3)	Br2–Sb1–Br4	88.36(2)
		Br2^{II}–Sb1–Br4	92.59(2)
Br3–Sb1–Br4	179.83(3)	Br3–Sb1–Br4	178.96(2)
Sb1–Br2–Sb1^{III}	164.75(5)	Sb1–Br2–Sb1^{III}	157.39(2)
C2–C1–N1	113.8(9)	C2–C1–N1	111.2(4)
C4–C3–N2	141.0(19)	C4–C3–N2	111.0(4)

Symmetry codes: (^{I}) $-x,y,z$; (^{II}) $x-1/2,y,-z+3/2$; (^{III}) $x+1/2,y,-z+3/2$.

Table 4. The D···A distances (Å) between anionic and cationic substructures of $(C_2H_5NH_3)_2[SbBr_5]$ at 298 K and 90 K.

298 K[a]		90 K	
N1···Br1^{I}	3.541(6)	N1···Br11^{IV}	3.450(4)
N1···Br4^{II}	3.421(7)	N1···Br4^{II}	3.380(4)
		N1···Br4^{I}	3.465(4)
N2···Br1	3.611(9)	N2···Br1	3.657(4)
–		N2···Br2	3.489(4)
N2···Br3^{III}	3.520(13)	N2···Br3^{III}	3.503(4)
		N2···Br3^{V}	3.499(4)

[a] One of two symmetry-related contacts is given.
Symmetry codes: (^{I}) $-x+1,-y+1,-z+2$; (^{II}) $-x+1/2,-y+1,z+1/2$; (^{III}) $x+1/2,-y+3/2,-z+2$; (^{IV}) $-x,-y+1,-z+2$; (^{V}) $x+1,y,z$.

2.998(1), while the shortest are 2.636(1) Å. The remaining two axial, terminal Sb–Br bonds have intermediate lengths, 2.769(1) and 2.790(1) Å. The Br–Sb–Br angles involving bromine atoms mutually *cis* range from 81.33(2) to 95.38(4)°, while those located *trans* are between 172.97(2) and 179.83(3)° (Table 3).

The same anionic substructure, built of $[SbBr_6]^{3-}$ octahedra connected by corners, was found in

Table 5. The hydrogen bond geometries (Å, °) for $(C_2H_5NH_3)_2[SbBr_5]$at 90 K.

D–H···A	D–H	H···A	D···A	D–H···A
N1–H11···Br11^{I}	0.89	2.67	3.450(4)	147
N1–H12···Br4^{II}	0.89	2.54	3.380(4)	157
N1–H13···Br4^{III}	0.89	2.60	3.465(4)	166
N2–H21···Br1	0.89	2.94	3.657(4)	139
N2–H23···Br2	0.89	2.68	3.489(4)	152
N2–H21···Br3^{IV}	0.89	2.82	3.503(4)	135
N2–H22···Br3^{V}	0.89	2.61	3.499(4)	173

Symmetry codes: (^{I}) $-x,-y+1,-z+2$; (^{II}) $-x+1/2,-y+1,z+1/2$; (^{III}) $-x+1,-y+1,-z+2$; (^{IV}) $x+1/2,-y+3/2,-z+2$; (^{V}) $x+1,y,z$.

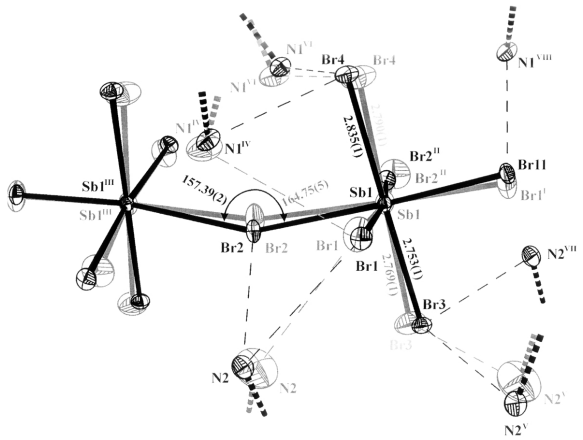

Fig. 3. Superposition of two corner-sharing $[SbBr_6]^{3-}$ octahedra with their neighbouring ethylammonium cations in the structures of bis(ethylammonium) pentabromoantimonate(III) at 298 (grey) and 90 K (black). Note the clear influence of the N···Br interactions on the geometrical parameters of the $[SbBr_6]^{3-}$ octahedra. The thin dashed lines denote the N···Br contacts. Displacement ellipsoids are plotted at the 25% and 50% probability level at 298 and 90 K, respectively. Symmetry codes: (^{I}) $-x,y,z$; (^{II}) $x-1/2,y,-z+3/2$; (^{III}) $x+1/2,y,-z+3/2$; (^{IV}) $-x+1,-y+1,-z+2$; (^{V}) $x-1/2,-y+3/2,-z+2$; (^{VI}) $-x+1/2,-y+1,z-1/2$; (^{VII}) $x-1,y,z$; (^{VIII}) $-x,-y+1,-z+2$.

the structure of $[H_3N(CH_2)_6NH_3][SbBr_5]$ [19] and $(C_5H_{12}N)_2[SbBr_5]$ [20]. In all the structures the Sb–Br bond lengths are in the same order. The longest are bridging, the shortest terminal opposite to bridging atoms and the remaining two terminal ones are of the intermediate length. The largest change, 0.127(4) Å, in Sb–Br bond lengths within the same type of central atom–ligand distances were found between bridging Sb–Br distances in the structure of the $(C_2H_5NH_3)_2[SbBr_5]$ and $(C_5H_{12}N)_2[SbBr_5]$ salts. Significant differences were noticed between both structures in the Br–Sb–Br angles involving bridg-

ing Br atoms. The largest dissimilarity, 13.3(2)°, was found for the inter-octahedral Sb–Br–Sb angle.

It is also worth to compare the deformation of the $[SbBr_6]^{3-}$ octahedron in the title structure with an isolated octahedron, not deformed by the formation of Sb–Br–Sb bridges. Lawton *et al.* reported the structure of pyridinium bromoantimonate containing Sb^{III} and Sb^{V} atoms, $(C_5H_5NH)_6Sb^{III}Sb^{V}{}_3Br_{24}$ [21] where the isolated $[SbBr_6]^{3-}$ octahedron was described. The Sb–Br distances, corrected for thermal effects assuming rigid-body libration of the ions, are between 2.793(7) and 2.809(10) Å. The average Sb^{III}–Br bond length is 2.799(7) Å and it is in agreement with other results [22, 23]. In our case the deformation of the inorganic chains is first of all related to the type of the anionic substructure. Therefore the largest difference, 0.199(8) Å, was noticed again for the bridging Sb–Br bond.

There are two crystallographically independent ethylammonium cations in the unit cell. Both cations occupy special positions and both are disordered. The type of disorder is similar for the two cations as realized by the presence of two positions of the methyl carbon atoms (Fig. 2). The geometrical parameters of the disordered ethylammonium cations are presented in Table 3. Because of the dynamical disorder the N–C, C–C bond lengths and N–C–C angles were not determined with a high precision.

Besides the interactions within the inorganic substructure, the N···Br contacts between oppositely charged moieties also contribute to the deformation of the $[SbBr_6]^{3-}$ polyhedra. The N···Br distances are between 3.421(7) and 3.611(9) Å. They are comparable to those found in other bromoantimonates(III) [*e.g.* 24, 25].

The observed changes in Sb–Br bond lengths and Br–Sb–Br angles correlate well with the distances and strengths of the N···Br interactions. The two axial distances are Sb1–Br3 (2.769(1) Å) and Sb1–Br4 (2.790(1) Å) since both axial atoms participate in the shortest N···Br interactions with ethylammonium cations. The N1···Br4 distance is shorter (by 0.099(20) Å) and in the consequence the Sb1–Br4 bond length is longer (by 0.021(2) Å) than Sb1–Br3 (Table 3, 4; Fig. 3).

Structure at 90 K

In the low-temperature phase of $(C_2H_5NH_3)_2[SbBr_5]$ all atoms are in general positions. One central Sb^{III} and five crystallographically independent Br atoms form the deformed $[SbBr_6]^{3-}$ octahedron. The infinitive $[\{SbBr_5\}^{2-}]_n$ chains built of corner-sharing octahedra are elongated, like in the structure at 298 K, along the *a* direction of the unit cell. The close relationship and the similarity of the corresponding unit cell parameters and the positions of the ionic components of the structures at both temperatures is obvious (Fig. 1).

The arrangement of the bromo ligands around the antimony(III) atom at 90 K deviates more strongly from the ideal octahedron than in the room-temperature phase. Pairs of Sb–Br bond lengths are in the same order like in the structure determined at 298 K. The lengths of the Sb–Br bonds vary from 2.609(1) to 3.057(1) Å. The difference between the shortest and the longest Sb–Br distances is 0.448(2) Å, while in the room-temperature structure it is 0.362(2) Å. A similar situation was noticed in the case of the *cis* Br–Sb–Br angles. The differences are 16.03(4)° and 14.05(6)° for the low- and room-temperature structure, respectively (Table 3).

Taking into account that in both phases the types of anionic and cationic substructures are the same, the differences described above are mainly related to two reasons: (I) the stereochemical activity of the lone electron pair located on the Sb^{III} atom [26, 27] and (II) the presence of N···Br interactions different in geometry and strength [*e.g.* 10].

The larger difference (0.082(2) Å) in the Sb–Br bond length of the axial Br3 and Br4 atoms at 90 K as compared to the structure at 298 K (0.021(2) Å) confirms again the influence of cationic substructure on the deformation of inorganic octahedra (Table 3 – 5; Fig. 3).

The largest changes in angles in both phases were found for the bridging Br2 atom. The Sb–Br2–Sb angle is decreased from 164.75(5) at 298 to 157.39(2)° at 90 K owing to the existence of the N–H···Br hydrogen bond in the phase below the transition temperature.

The conclusion to be drawn from the results is that the rather weak interionic interactions as well as hydrogen bonds, formed between Br atoms and ethylammonium cations, have relatively strong influence on the deformation of the $[SbBr_6]^{3-}$ octahedra, especially in the case of the geometrical parameters related to bridging, the furthest from the central atom located, ligands.

The bond lengths and angles of the ethylammonium cation are typical (Table 3). They are similar to those

found in the structure of ethylamine dibromide [28]. All geometric parameters of the $(C_2H_5NH_3)^+$ ion in the low-temperature phase of $(C_2H_5NH_3)_2[SbBr_5]$ are also in a good agreement with those reported in the $(C_2H_5NH_3)_2[SbCl_5] \cdot (C_2H_5NH_3)Cl$ chloroantimonate(III) at 90 K [6].

Phase transition

A characteristic feature of halogenoantimonates(III) and halogenobismuthates(III) are the molecular dynamics of the organic cations embedded in the anionic substructures. It is especially manifested with relatively small methyl-, dimethyl-, trimethyl- and tetramethylammonium cations. On decreasing the temperature the reorientations of the cations are frozen, which may lead to one or more phase transitions [29, 30]. There are a few examples of bromoantimonates(III) with organic cations of the R_2SbBr_5 stoichiometry in which phase transitions were detected [16, 31].

Nuclear quadrupole resonance (NQR), differential thermal analysis (DTA) and nuclear magnetic resonance (NMR) studies of the title compound have shown that it undergoes a low-temperature phase transition at *ca.* 155 K (NQR studies – changing the slope of the ^{81}Br resonance lines) [32]. On the basis of the temperature dependence of the second moments of the ^1H NMR line performed between 290 and 125 K, the rapid decrease of the second moment in the vicinity of 150 K was considered to be due to the freezing of motions of the ethylammonium cation around its long axis.

The results of our DSC studies are generally in agreement with the DTA measurements reported by Okuda *et al.* [32], who found that the temperature of transition during cooling and heating of the sample was 155.1 and 157.2 K, respectively. The DSC diagram in cooling and heating runs for $(C_2H_5NH_3)_2[SbBr_5]$ reveals also one distinct thermal anomaly at *ca.* 158.5 K (158 K in cooling and 159 K in heating run). The enthalpy and entropy of the transition are $\Delta H = 0.4$ kJ $\cdot$ mol^{-1} and $\Delta S = 2.7$ J $\cdot$ mol$^{-1}\cdot$ K^{-1}, respectively.

The results of the X-ray single crystal measurements described above confirm that the mechanism of the phase transition in the title salt is connected with changes in motions of the cationic substructure. The observed disorder of the methyl carbon atoms, together with relatively large thermal motions, are reflected in the high displacement parameters of the remaining C and N atoms of two crystallographically independent ethylammonium cations in the room-temperature phase. It clearly suggests that the molecules reorient along their long axis (Fig. 2). In the low-temperature phase, *ca.* 70 K below the temperature of transition, the molecular motions of the organic cations are frozen.

Experimental Section

Synthesis and characterization

Antimony(III) oxide (pure, Ubichem Ltd., UK), ethylamine (for synthesis, 70%, Merck-Schuchardt, Germany) and concentrated hydrobromic acid (A.C.S reagent, 48%, Aldrich, Germany) were the starting materials used for the synthesis of bis(ethylammonium) pentabromoantimonate(III).

Single crystals suitable for the X-ray diffraction studies of bis(ethylammonium) pentabromoantimonate(III) were grown by slow evaporation of the solvent at the room temperature from a saturated solution obtained in the reaction of 2.91 g (10 mmol) Sb_2O_3 and 12.88 ml (160 mmol) $C_2H_5NH_2$ in a concentrated hydrobromic acid (*ca.* 60 ml). The solution was heated and stirred till the antimony(III) oxide and then the product of the reaction was completely dissolved.

The TGA studies were performed on a Universal V1.12A TA Instrument in the temperature range 300 – 630 K (rate 10 K $\cdot$ min^{-1}). The macrocrystalline sample was ground before the measurements.

The differential scanning calorimetry (DSC) studies were carried out on a Perkin-Elmer DSC-7 calorimeter with a cooling/heating rate of 20 K $\cdot$ min^{-1} in the temperature range 100 – 443 K.

Crystal structure determinations

The measurements at 298 and 90 K were performed on a Xcalibur CCD diffractometer with graphite monochromated Mo-K$_\alpha$ ($\lambda = 0.71073$ Å) radiation. At 90 K the intensity data were collected on the diffractometer equipped with an Oxford Cryosystems cooler. The reflections were measured using the ω-scan technique with $\Delta\omega = 0.50$ and 0.75°. The unit cell parameters were obtained from a least squares refinement of 1379 and 2641 reflections at 298 and 90 K, respectively.

Both structures were solved by the Patterson method. All data were subjected to Lorentz, polarisation and empirical absorption corrections based on symmetry-equivalent reflections [33] ($T_{min} = 0.144$, $T_{max} = 0.327$ and $T_{min} = 0.119$, $T_{max} = 0.176$ for the measurements at 298 and 90 K, respectively).

Fourier maps revealed a dynamical disorder of both crystallographically independent ethylammonium cations at

298 K and we were thus not able to find the positions of hydrogen atoms. All hydrogen atoms of the low-temperature structure were located in subsequent maps and then refined using the riding model and constrained to a distance of 0.96, 0.97 and 0.89 Å for $–CH_3$, $–CH_2–$ and $–NH_3$ groups respectively. The hydrogen atoms of the methyl and ammonium groups were allowed to ride on the C and N atoms and to rotate around the neighbouring C–C and C–N bonds. Their displacement parameters were taken with coefficients 1.3, 1.2 and 1.5 times larger than the respective parameters of the nitrogen, methylene and methyl carbon atoms.

The quantity minimised was $\Sigma w(|F_o| - |F_c|)^2$ with the weighting scheme $w = 1/[\sigma^2(F_o^2) + (0.0462P)^2]$ and $w = 1/[\sigma^2(F_o^2) + (0.0181P)^2]$ $(P = (F_o^2 + 2F_c^2)/3)$ at 298 and 90 K, respectively.

The Oxford Diffraction software CrysAlisCCD and CrysAlisRED programs were used during the data collection, cell refinement and data reduction processes [34]. The SHELX-97 program [35] was used for the structure solution and refinement. The structure drawings were prepared using SHELXTL program [33].

Crystallographic data (excluding structure factors) for bis(ethylammonium) pentabromoantimonate(III) at 298 and 90 K have been deposited at the Cambridge Crystallographic Data Centre as supplementary publication nos. CCDC 211366 and CCDC 211367, respectively. Copies of the data can be obtained, free of charge, on application to the Director, CCDC, 12 Union Road, Cambridge CB2 1EZ, UK (Fax: int. code+(1223) 336033 or e-mail: data_request@ccdc.cam.ac.uk).

[1] M. Bujak, J. Zaleski, Acta Crystallogr. **C55**, 1775 (1999).
[2] M. Bujak, L. Sikorska, J. Zaleski, Z. Anorg. Allg. Chem. **626**, 2535 (2000).
[3] M. Bujak, J. Zaleski, Cryst. Eng. **4**, 241 (2001).
[4] M. Bujak, J. Zaleski, Acta Crystallogr. **C54**, 1773 (1998).
[5] M. Bujak, J. Zaleski, Z. Naturforsch. **56b**, 521 (2001).
[6] M. Bujak, J. Zaleski, Pol. J. Chem. **73**, 773 (1999).
[7] M. Bujak, J. Zaleski, Z. Naturforsch. **55a**, 526 (2000).
[8] J. A. Hayes, J. Amer. Chem. Soc. 360 (1902).
[9] R. D. Whealy, R. L. Yeakley, J. Inorg. Nucl. Chem. **25**, 365 (1963).
[10] J. M. Stewart, K. L. McLaughlin, J. J. Rossiter, J. R. Hurst, R. G. Haas, V. J. Rose, B. E. Ciric, J. A. Murphy, S. L. Lawton, Inorg. Chem. **13**, 2767 (1974).
[11] N. K. Jha, S. S. A. Rizvi, J. Inorg. Nucl. Chem. **38**, 401 (1976).
[12] N. K. Jha, S. S. A. Rizivi, J. Inorg. Nucl. Chem. **34**, 2953 (1972).
[13] N. K. Jha, S. S. A. Rizivi, J. Inorg. Nucl. Chem. **36**, 1479 (1974).
[14] G. C. Allen, R. F. McMeeking, Inorg. Chim. Acta **23**, 185 (1977).
[15] M. J. F. Leroy, G. J. Goetz, Bull. Chim. Soc. Fr., 120 (1979).
[16] T. Okuda, N. Tanaka, S. Ichiba, K. Yamada, Z. Naturforsch. **41a**, 319 (1986).
[17] R. Jakubas, L. Sobczyk, J. Matuszewski, Ferroelectrics **74**, 339 (1987).
[18] M. Bujak, Ph. D. Thesis, University of Opole, Opole, Poland (2000).
[19] G. A. Mousdis, G. C. Papavassiliou, A. Terzis, C. P. Raptopulou, Z. Naturforsch. **53b**, 927 (1998).
[20] A. Abdel-Rehim, E. A. Meyers, Cryst. Struct. Commun. **2**, 45 (1973).
[21] S. L. Lawton, R. A. Jacobson, R. S. Frye, Inorg. Chem. **10**, 701 (1971).
[22] S. L. Lawton, R. A. Jacobson, Inorg. Chem. **10**, 709 (1971).
[23] T. Okuda, M. Hiura, E. Koshimizu, H. Ishihara, Y. Kushi, H. Negita, Chem. Lett. 1321 (1982).
[24] H. Ishihara, S. Dou, A. Weiss, Bull. Chem. Soc. Jpn. **67**, 637 (1994).
[25] J. M. Carola, D. D. Freedman, K. L. McLaughlin, P. C. Reim, W. J. Schmidt, R. G. Haas, W. J. Broome, E. A. DeCarlo, S. L. Lawton, Cryst. Struct. Commun. **5**, 393 (1976).
[26] R. J. Gillespie, Chem. Soc. Rev. **59** (1992).
[27] X. Wang, F. Liebau, Acta Crystallogr. **B52**, 7 (1996).
[28] F. Jellinek, Acta Crystallogr. **11**, 626 (1958).
[29] R. Jakubas, L. Sobczyk, Phase Trans. **215**, 97 (1990).
[30] L. Sobczyk, R. Jakubas, J. Zaleski, Pol. J. Chem. **71**, 265 (1997).
[31] R. Jakubas, G. Bator, M. Foulon, J. Lefebvre, J. Matuszewski, Z. Naturforsch. **48a**, 529 (1993).
[32] T. Okuda, Y. Kinoshita, H. Terao, K. Yamada, Z. Naturforsch. **49a**, 185 (1994).
[33] G. M. Sheldrick, SHELXTL. Siemens Analytical X-ray Instrument Inc., Madison, Winsconsin, USA (1990).
[34] Oxford Diffraction; CrysAlis CCD, Data collection GUI for CCD and CrysAlis RED, CCD data reduction GUI versions 1.169.5 and 1.170.16, Oxford Diffraction Poland (2002).
[35] G. M. Sheldrick, SHELX-97. Program for the Solution and the Refinement of Crystal Structures. University of Göttingen, Germany (1997).